[structure factor table]
(Chapter 5.4.3 in *Elements*)

Structure Factors

Table 5-U1. STRUCTURE FACTORS PER CELL OF MONATOMIC CUBIC CRYSTALS

Crystal	Atoms per cell	Structure factor F_{hkl}	Indices h, k, l
BCC	2	2	h + k + l even
		0	h + k + l odd
FCC	4	4	h, k, l all even or all odd
		0	h, k, l mixed even or and odd
Diamond	8	0	h, k, l mixed even or and odd
		8	h + k + l = 4n (even and exactly divisible by 4)
		0	h + k + l = even but not 4n
		4(1 ± i)	h + k + l = odd; $\lvert F_{hkl}\rvert = 4\sqrt{2}$; i = √(-1))

In *m*-fold multibounce crystals, the reflectivity function for either case is

$$R_m(\lambda,\theta) = R_1^m(\lambda,\theta) \tag{5-U6}$$

and within the range of the plateau, $R_1^m = 1$.

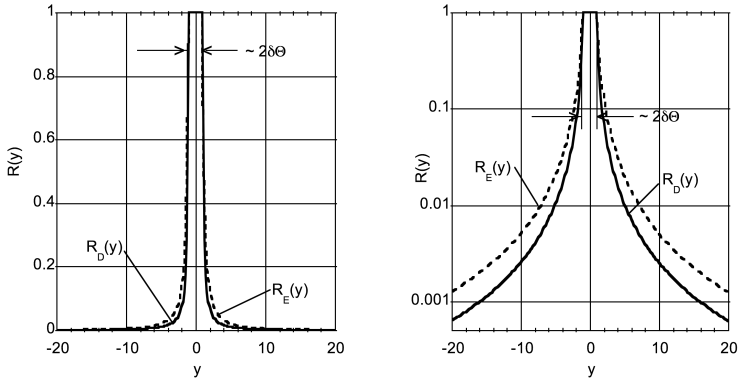

Figure 5-U2. The Darwin and Ewald reflectivity functions for non-absorbing crystals.

The reflectivity functions are often idealized as top-hat functions $2\delta\theta_D$ wide, with no wings. However, the wings dominate the reflectivity for large *y*. The table gives structure factors for different classes of reflections *hkl* in diamond-structure crystals.

[USANS vs. conventional SANS]
(Chapter 5.4.3 in *Elements*)

USANS Vs. Conventional SANS

Figure 5-UvsC1 shows schematically a double-crystal diffractometer based on these principles.

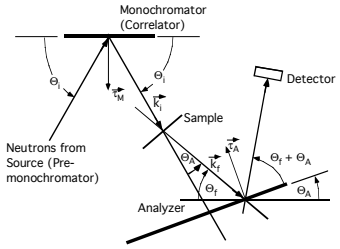

Figure 5-UvsC1. Schematic diagram showing the propagation of neutrons through the double-crystal arrangement. The angles between the incident and scattered wave vectors and the offset angle Θ_A are greatly exaggerated in the figure.

The scattered-neutron counting rate for given offset angle θ_A and wavelength λ is

$$C(\Theta_A, \lambda) = \int A(\theta_i, \lambda) R(\Theta_i - \Theta_B, \lambda) S\left[Q(\Theta_i - \Theta_f, \lambda)\right] R(\Theta_f + \Theta_A - \Theta_B, \lambda) d\Theta_i d\Theta_f, \tag{5-UvsC1}$$

where $R(\theta,\lambda)$ is the reflectivity function and $A(\theta_i,\lambda)$ is the incident intensity. Expressed in terms of the *resolution function*, the convoluton of two $R(\theta,\lambda)$ functions, is

$$I(\psi, \lambda) = \int A(\phi + \Theta_B, \lambda) R(\phi, \lambda) R(\phi - \psi, \lambda) d\phi, \tag{5-UvsC2}$$

so that the counting rate, now including the full accepted λ range, is

$$C(\Theta_A) = \int I(\psi, \lambda) S\left[Q(\Theta_A + \psi, \lambda)\right] d\lambda d\psi, \tag{5-UvsC3}$$

which is a slit-smeared, broadened version of the scattering function. The minimum value of Q that is accessible without the resolution function overlapping the transmitted unscattered beam is $Q_{\min} = 4\pi\delta\theta_D / \lambda$.

Exercise. Calculate Q_{min} for 3.6-Å neutrons scattered at Bragg angle 70° from the 220 reflection of 300-K silicon.

The resolution function for an *m*-bounce DCD is approximately triangular when the reflectivity functions are approximated as top-hat functions. Ignoring the wavelength dependence and the illumination factor, the resolution function is

$$I_m(\Delta) = \int R^m(y) R^m(y - \Delta) dy \,, \qquad \text{(5-UvsC4)}$$

in which the wings approach Δ^{-2m} and enable small-angle scattering measurements at very small Q-values. The principle works for both neutrons and x rays.

The counting rate distribution due to neutrons passing through the sample without interaction (unscattered neutrons) accompanies the scattered-neutron distribution and for small scattering angles dominates the observation. The unscattered component has the same form as previously shown, with a δ-function $T\delta(\theta_i - \theta_f)$ replacing the sample scattering function S(Q). Measurement without the sample provides the shape of the unscattered component, which is the resolution function, or the *rocking curve*. In practice, the unscattered component, normalized by the factor T, is subtracted from the sample-in data to provide the measured scattering function. The transmitted fraction, T, is determined from separate measurements of the beam from the monochromator crystal with and without the sample.

When the second crystal is offset by angle θ_A, the first and second crystal reflections overlap, sampling the scattering at angle θ_A. Ignoring the wings on the reflectivity functions, we have a triangular weighting function, the resolution function, which is the convolution of the two rectangular functions, extending in bands along the locus $\lambda = 2d \sin \Theta$. The full width at half-maximum (FWHM) of the triangular distribution as a function of y is $2\delta\Theta_D$. Figure 14 shows the DCD rocking curve (resolution function). If the wings of the reflectivity function were accounted for, the rocking curve would show similar wings extending beyond the limits of the triangular function.

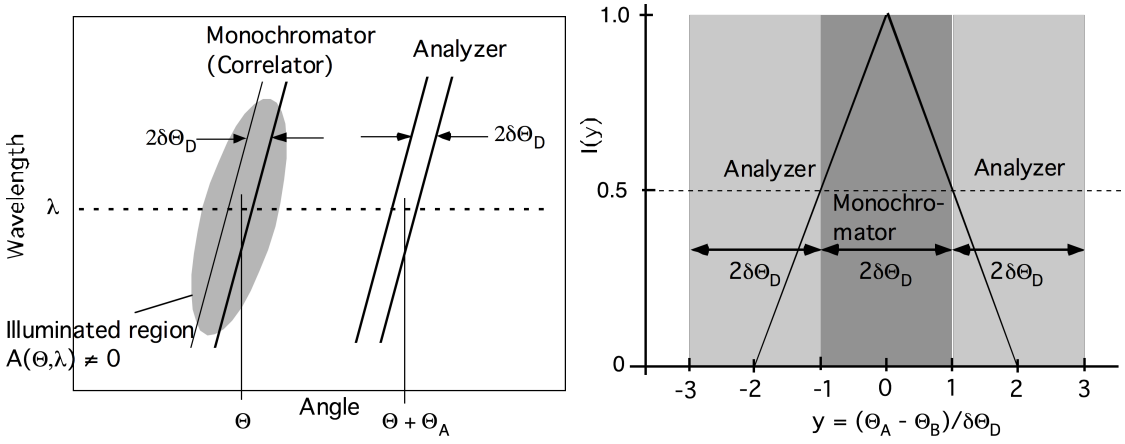

Figure 5-UvsC2. Left. The accepted wavelength and angle bands of the monochromator (correlator) and the analyzer. Right. The triangular rocking curve (resolution function) of the diffractometer, the convolution of two rectangular (top hat) functions, as a function of the offset angle Θ_A.

The minimum value of Q that is accessible without the resolution function overlapping the transmitted unscattered beam is $Q_{min} = 4\pi\delta\Theta_D/\lambda$, as is evident from Fig. 5-UvsC2.

Deconvoluting the resolution smearing

The USANS technique disperses the scattering only in the plane of reflection, averaging over the measured function in the direction perpendicular to the scattering plane and producing a *slit-camera i. e., a Kratky camera* image. The angle integrals are multidimensional—the angle distributions depend on details of the collimation. The slit-smeared function $I_s(Q)$ is related to the *point geometry* image $I_p(Q)$ as

$$I_s(Q) = \int\int W_h(t) W_v(u) I_p\left\{\frac{2\pi}{\lambda}\left[(2\theta - t)^2 + u^2\right]^{1/2}\right\} du dt, \qquad \text{(5-UvsC5)}$$

where the angle distributions $W_h(t)$ and $W_v(u)$, normalized to unit area, are respectively the horizontal and vertical collimation functions for angles t and u, $Q = \frac{2\pi}{\lambda}\sin(\theta)$, and 2θ is the scattering angle.

Mathematical inversion produces the conventional point-geometry function from the measured slit-smeared function but the convolution-like form is not amenable to direct methods. Feigin and Svergun (1987) discuss this data treatment in detail. In contrast to SANS measurements (point geometry), USANS measurements cannot be interpreted simply by fitting parameters in tabulated point-scattering functions; see *Elements,* Chapter 14.9.1 and Pedersen 1997. This is because the broadening functions W_h and W_v in Eq. 5-UvsC5 depend on specifics of each instrument and beyond the scope of this discussion. Therefore for USANS this process is usually carried out by optimized cut-and-try modeling methods.

References

Feigin, L. A. and D. I. Svergun (1987). *Structure Analysis by Small-Angle X-ray and Neutron Scattering*. Plenum Press, ch. 9, p. 277 ff.

Pedersen, J. S. (1997). Analysis of small-angle scattering data from colloids and polymer solutions: modeling and least squares fitting. *Adv. Colloid Interfac.***70**, 171.